

Spin Qubits in Multi-Electron Quantum Dots

Serguei Vorojtsov,¹ Eduardo R. Mucciolo,^{1,2} and Harold U. Baranger¹

¹*Department of Physics, Duke University, Box 90305, Durham, North Carolina 27708-0305*

²*Departamento de Física, Pontifícia Universidade Católica do Rio de Janeiro, C.P. 37801, 22452-970 Rio de Janeiro, Brazil*

(Dated: June 4, 2018)

We study the effect of mesoscopic fluctuations on the magnitude of errors that can occur in exchange operations on quantum dot spin-qubits. Mid-size double quantum dots, with an odd number of electrons in the range of a few tens in each dot, are investigated through the constant interaction model using realistic parameters. It is found that the constraint of having short pulses and small errors implies keeping accurate control, at the few percent level, of several electrode voltages. In practice, the number of independent parameters per dot that one should tune depends on the configuration and ranges from one to four.

PACS numbers: 03.67.Lx, 73.21.La

Keywords: quantum computation, quantum dots, qubits, gate errors

I. INTRODUCTION

Since the discovery that quantum algorithms can solve certain computational problems much more efficiently than classical ones,^{1,2} attention has been devoted to the physical implementation of quantum computation (QC). Among the many proposals, there are those based on the spin of electrons in laterally confined quantum dots (QD),³ which may have great potential for scalability and integration with current technologies. For any successful proposal, one must be able to perform single- and double-qubit operations much faster than the decoherence time. In fact, all logical operations required for QC can be realized if these elementary operations are sufficiently error free.⁴

Single qubit operations involving a single QD will likely require precise engineering of the underlying material or control over local magnetic fields;⁵ both have yet to be achieved in practice. Two-qubit operations, in contrast, are already within experimental reach. They can be performed by sending electrical pulses to modulate the potential barrier between adjacent QDs. That permits direct control over the effective, Heisenberg-like, exchange interaction between the qubit spins, which is created by the overlap between the electronic wave-functions of the QDs.³ These operations are important elements in forming a basic two-qubit gate such as the controlled-not⁶ and in the propagation of quantum information through QD arrays.³ In fact, using three QDs instead of just one to form a logical qubit would allow one to perform all logical operations entirely based on the exchange interaction.⁷ Thus, exchange operations will likely play a major role in the realization of QD qubits. A quantitative understanding of errors that occur during an exchange operation will help in designing optimal systems.

The first proposal for a QD spin qubit³ relied on having a single electron in a very small laterally confined QD. One advantage of such a system is that the Hilbert space is nominally two-dimensional. Leakage from the computational space involves energies of order either the charging energy or the single-particle excitation energy, both of which are quite large in practice (~ 1 meV

~ 10 K). Working adiabatically – such that the inverse of the switching time is much less than the excitation energy – assures minimal leakage. The large excitation energy implies that pulses of tens of picoseconds would be both well within the adiabatic regime and below the dephasing time τ_ϕ (which is typically in the nanosecond range since orbital degrees of freedom are involved). However, in practice, it is difficult to fabricate very small tunable devices.⁸ Moreover, one-electron QDs may offer little possibility of gate tuning due to their rather featureless wave functions.

Alternatively, a qubit could be formed by the top most “valence” electron in a QD with an odd number of electrons.⁹ In this case, electrons filling the lower energy states should comprise an inert shell, leaving as the only relevant degree of freedom the spin orientation of the valence electron. Large QDs with 100-1000 electrons, while much simpler to fabricate than single electron QDs, are unsuitable because the excitation energy is small ($\sim 50 \mu\text{eV} \sim 0.6$ K), leading to leakage or excessively slow exchange operations. On the other hand, mid-size QDs, with 10-40 electrons, are sufficiently small to have substantial excitation energies, yet both reasonable to fabricate and tunable through plunger electrodes. For these dots, a careful analysis of errors is necessary.

Perhaps the best example of an exchange operation is the swap of the spin states of the two qubits. For instance, it causes up-down spins to evolve to down-up. Maximum entanglement between qubits occurs when half of a swap pulse takes place – a square-root-of-swap operation. Several authors have treated the problem of swap errors in QD systems.^{10,11,12,13,14} A primary concern was the occurrence of double occupancy (when both valence electrons move into the same QD) during and after the swap. However, no study so far has considered another intrinsic characteristic of electronic states in multi-electron QDs, namely, their marked dependence on external perturbations such as electrode voltage or magnetic field. This sensitivity gives rise to strong sample-to-sample fluctuations arising from the phase-coherent orbital motion.¹⁵ These features can make the precise control of energy levels, wave functions, and inter-dot

couplings a difficult task.

In this work we study errors and error rates that can take place during the exchange operation of two spin qubits based in multi-electron QDs. We consider realistic situations by taking into account an extra orbital level and fluctuations in level positions and coupling matrix elements. These lead to deviations from a pre-established optimal swap operation point, especially when a single-particle level falls too close to the valence electron level. Reasons for such fluctuations can be, for instance, (i) the lack of a sufficient number of tuning parameters (i.e., plunger electrodes), or (ii) the cross-talk between the tuning electrodes. Our results set bounds on the amount of acceptable detuning for mid-size QD qubits.

This paper is organized as follows. In Sec. II, we introduce and justify the model Hamiltonian. The states involved in the exchange operation are presented in Sec. III, where we also discuss the pulses and the parameters involved in the exchange operations. In Sec. IV we present the results of our numerical simulations. We also discuss the impact of mesoscopic effects on errors and put our analysis in the context of actual experiments. Finally, in Sec. V we draw our conclusions.

II. MODEL SYSTEM

We begin by assuming that the double QD system can be described by the Hamiltonian¹⁶

$$H = H_A + H_B + H_{AB}, \quad (1)$$

where

$$H_\alpha = \sum_{j,\sigma} \epsilon_j^\alpha n_{\alpha,j\sigma} + \frac{U_\alpha}{2} \sum_{j,\sigma} n_{\alpha,j\sigma} \left(\sum_{k,\sigma'} n_{\alpha,k\sigma'} - 1 \right), \quad (2)$$

$\alpha = A, B$, and

$$H_{AB} = \sum_{j,k,\sigma} \left(t_{jk} a_{j\sigma}^\dagger b_{k\sigma} + \text{h.c.} \right). \quad (3)$$

Here, $n_{A,j\sigma} = a_{j\sigma}^\dagger a_{j\sigma}$ and $n_{B,k\sigma} = b_{k\sigma}^\dagger b_{k\sigma}$ are the number operators for the single-particle states in the QDs (named A and B), ϵ_j^α denotes the single-particle energy levels, t_{jk} are the tunneling amplitudes between the dots, and U_α is the charging energy ($\sigma = \uparrow, \downarrow$ and j, k run over the single-particle states). Typically, for mid- to large-size QDs, the charging energy is larger than the mean level spacing.

In the literature of Coulomb blockade phenomena in closed QDs, the Hamiltonian in Eq. (2) is known as the constant interaction model. It provides an excellent description of many-electron QDs, being supported by both microscopic calculations and experimental data.^{15,16,17,18,19} The reasoning behind its success can be understood from two observations. First, mid- to large-size QDs, with more than ten electrons, behave very much like conventional disordered metals in the diffusive

regime. Wavelengths are sufficiently small to resolve irregularities in the confining and background potentials, leading to classical chaos and the absence of shell effects in the energy spectrum. In this case, the single-particle states obey the statistics of random matrices, showing complex interference patterns and resembling a random superposition of plane waves. This is in contrast with the case of small, circularly symmetric, few-electron QDs, where shell effects are pronounced.^{9,20}

Second, for realistic electron densities, the QD linear size is larger than the screening length of the Coulomb interactions. In the presence of random plane waves, the screened interaction can then be broken up into a leading electrostatic contribution characterized by the QD capacitance plus weak inter-particle residual interactions.^{16,19} This description becomes more accurate as the number of electrons gets larger since the residual interactions become weaker. The electron bunching is reduced as wave functions become more uniformly extended over the QD. Also, the increase in the number of oscillations in the wave functions leads to a self-averaging of the residual interactions. In this limit, one arrives at the so-called “universal Hamiltonian” for QDs, containing only single-particle levels, the charging energy, and a mean-field exchange term.^{15,16} This Hamiltonian can be derived explicitly via a random-phase approximation treatment of the Coulomb interaction and the use of random-matrix wave functions.^{16,19}

According to these arguments, interaction effects beyond the charging energy term are omitted in Eq. (2). In addition, the intra-dot exchange interaction, which tends to spin polarize the QD, is also neglected. The reason for that is the following. One can show that the intra-dot exchange term only affect states where there is double occupancy of a level. Thus, the exchange interaction constant always appears side-by-side with the charging energy. But in multi-electron dots, the exchange energy (which is at most of order of the mean level separation) is much smaller than the charging energy. Thus, intra-dot exchange effects are strongly suppressed by the charging energy. We have verified that their inclusion does not modify appreciably our final results. We expect the exchange interaction to become important for two-qubit operations only in the case of small QDs with only a few electrons, when all energy scales (including the mean level spacing) are of the same order.

Thus, the simple picture where single-particle states are filled according to the Pauli principle up to the top most level is an appropriate description of multi-electron dots.^{15,16,17,18,19} In order to define the spin- $\frac{1}{2}$ qubits, both QDs should contain an odd number of electrons (say, $2N_A - 1$ and $2N_B - 1$). The QD spin properties are then dictated by the lone, valence electron occupying the highest level. The remaining electrons form an inert core, provided that operations are kept sufficiently slow so as not to cause particle-hole excitations to other levels.

Experimentally, the two-qubit exchange operations also require the capability of isolating the QDs from each

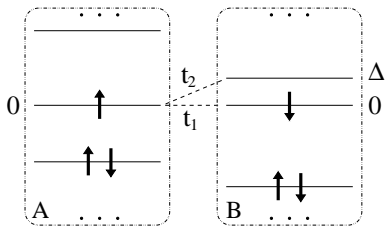


FIG. 1: Schematic disposition of energy levels of a system of two QD spin qubits (only levels close to the top occupied state are shown). The dashed lines indicate the most probable transitions that can occur during the exchange operation.

other, so that a direct product state can be prepared, such as

$$|i\rangle = |N_A, \uparrow\rangle_A \otimes |N_B, \downarrow\rangle_B, \quad (4)$$

where the kets represent only the spin of the valence electron on each QD.

III. ERRORS IN EXCHANGE OPERATIONS

We focus our study on errors that appear after a full swap operation (which should result in no entanglement). Although it could in principle seem more sensible to look at the square-root-of-swap operation (which creates entanglement and is therefore a building block of logical gates), error magnitudes for the latter are straightforwardly related to those of the full swap operation, as we will show. We leave the discussion of the square root of swap to Sec. IV.

The ideal full swap operation exchanges the valence electrons of the QD system. For instance, it takes the product state $|i\rangle$ into

$$|f\rangle = \hat{U}_{\text{sw}} |i\rangle = |N_A, \downarrow\rangle_A \otimes |N_B, \uparrow\rangle_B. \quad (5)$$

Physically, the full swap can be implemented by starting with isolated QDs, turning on the inter-dot coupling for a time T (the pulse duration), and then turning it off, isolating the QDs again. For weakly coupled QDs ($|t| \ll U, \delta\epsilon$), one finds $T \approx (\pi/4)U/|t|^2$, where t and U here represent typical values for the coupling matrix element and the charging energy, respectively (throughout we assume $\hbar = 1$). To quantify the amount of error that takes place during the operation, we use the probability of not reaching $|f\rangle$ asymptotically, namely,

$$\varepsilon = 1 - |\langle f | \psi(+\infty) \rangle|^2. \quad (6)$$

We solved numerically the time-dependent Schrödinger equation that derives from Eq. (1) for the particular but nevertheless realistic case shown in Fig. 1. We assumed that voltage tuning allows one to place the top most electron of QD A into an isolated single-particle state of energy $\epsilon_{N_A}^A = 0$ aligned with the energy of the top most electron in QD B , $\epsilon_{N_B}^B = 0$. However, limited tuning ability leaves an adjacent empty state close in energy in QD

B : $\epsilon_{N_B+1}^B = \Delta$. Therefore, while we can approximately neglect all levels but one in QD A , for QD B we needed to take two levels into account, having hopping matrix elements denoted by $t_1 = t_{N_A N_B}$ and $t_2 = t_{N_A, N_B+1}$.²¹ To facilitate the analysis, we assumed that the dots have the same capacitance, C , so that $U_A = U_B = U = e^2/C$.

The Hamiltonian of Eq. (1) conserves total spin. Assuming that filled inner levels in both QDs are inert (forming the “vacuum” state $|0\rangle$), we can span the $S_z = 0$ Hilbert subspace with nine two-electron basis states. According to their transformation properties, they can be divided into “singlet”

$$\begin{aligned} |S_l\rangle &= \frac{1}{\sqrt{2}} \left(b_{N_B+l-1, \downarrow}^\dagger a_{N_A \uparrow}^\dagger - b_{N_B+l-1, \uparrow}^\dagger a_{N_A \downarrow}^\dagger \right) |0\rangle, \\ |D_l\rangle &= b_{N_B+l-1, \downarrow}^\dagger b_{N_B+l-1, \uparrow}^\dagger |0\rangle, \\ |D_3\rangle &= \frac{1}{\sqrt{2}} \left(b_{N_B+1, \downarrow}^\dagger b_{N_B \uparrow}^\dagger - b_{N_B+1, \uparrow}^\dagger b_{N_B \downarrow}^\dagger \right) |0\rangle, \\ |D_4\rangle &= a_{N_A \downarrow}^\dagger a_{N_A \uparrow}^\dagger |0\rangle, \end{aligned} \quad (7)$$

and “triplet”

$$\begin{aligned} |T_l\rangle &= \frac{1}{\sqrt{2}} \left(b_{N_B+l-1, \downarrow}^\dagger a_{N_A \uparrow}^\dagger + b_{N_B+l-1, \uparrow}^\dagger a_{N_A \downarrow}^\dagger \right) |0\rangle, \\ |D_5\rangle &= \frac{1}{\sqrt{2}} \left(b_{N_B+1, \downarrow}^\dagger b_{N_B \uparrow}^\dagger + b_{N_B+1, \uparrow}^\dagger b_{N_B \downarrow}^\dagger \right) |0\rangle, \end{aligned} \quad (8)$$

classes, with $l = 1, 2$.

The final states that correspond to an error have either double occupancy ($|D_k\rangle$, $k = 1, \dots, 5$), or an electron in the $(N_B + 1)$ -level of QD B ($|S_2\rangle$ and $|T_2\rangle$).²² In addition, a return to the initial state is also considered an error. It is worth noticing the difference between our treatment of the problem and that of Ref. 13. In our case, errors come mainly from either ending in the excited single-particle state after the operation is over (i.e., states $|S_2\rangle$ and $|T_2\rangle$), or from “no-go” defective operations. In Ref. 13, errors come from having double occupancy in the final state. Double occupancy errors can be exponentially suppressed by adiabatically switching the pulse on and off on time scales larger than the inverse charging energy.^{3,11,13} Making pulses adiabatic on the time scale of the inverse mean level spacing for multi-electron quantum dots is more challenging, especially because the spacings fluctuate strongly both from quantum dot to quantum dot and upon variation of any external parameter (mesoscopic fluctuations). Therefore, multi-electron quantum dots require extra tunability to get around such problems.

Very small errors, below 10^{-6} – 10^{-4} , can, in principal, be fixed by the use of error correction algorithms.²³ The pulses, therefore, should be sufficiently adiabatic for errors to remain below this threshold. We adopted the following pulse shape:

$$v(t) = \frac{1}{2} \left(\tanh \frac{t+T/2}{2\tau} - \tanh \frac{t-T/2}{2\tau} \right), \quad (9)$$

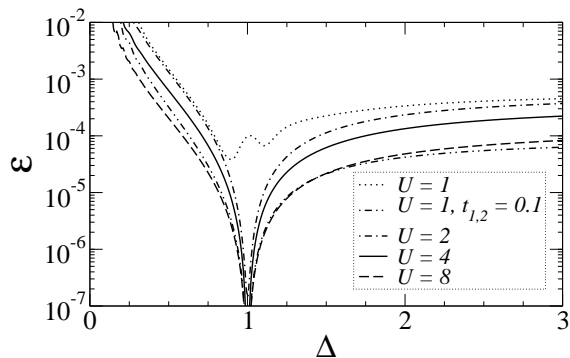


FIG. 2: Full swap error as a function of upper level detuning in quantum dot B . The pulse width is optimized for $\Delta = 1$, $\tau = 6$, and $t_{1,2} = 0.2$. Results for different charging energies are shown. Interference between different quantum mechanical paths in the device causes a sharp minimum.

where τ is the switching time. The pulse will remain both well-defined and adiabatic provided that $T \gg \tau \gg \max\{\Delta^{-1}, U^{-1}\}$. Notice that this pulse is equivalent to that adopted in Ref. 13 up to exponential accuracy, $O(e^{-T/\tau})$, with $T \gg \tau$. There is no particular reason to believe that either performs better than the other; our choice was dictated by technical convenience.

IV. RESULTS

We used a standard numerical method, the so-called Richardson extrapolation,²⁴ to solve the Schrödinger equation for $|\psi(t)\rangle$. The first step in our analysis was to find the optimal value of T which minimized the full swap error, as defined in Eq. (6), for a given set of parameters U , t_1 , and τ (we used $\Delta = 1$ and took $t_2 = t_1$). The second step was to study how this minimal error depends on τ . There is actually an optimal interval for τ , since small switching times spoil adiabaticity, while large ones compromise the pulse shape (when T is relatively short). Empirically, we find that errors related to switching times become negligible once τ reaches values of about $\tau_0 = 4 \max\{\Delta^{-1}, U^{-1}\}$, provided that $\tau \ll T$. In what follows, we fix $\tau \geq \tau_0$.

A. Mesoscopic Effects

Figure 2 shows the full swap error as a function of Δ when T is fixed to its optimal value for $\Delta = 1$. Such a situation would arise experimentally if the pulse is optimized for a certain configuration, but a fluctuation in level spacing occurs. Notice the sharp increase in error as Δ decreases. While increasing τ reduces this error (by making the switching more adiabatic), very small level spacings would be problematic, since τ can not be larger than T without sacrificing pulse shape and effectiveness. In order to make space for an adiabatic switching time for small Δ , one would also have to increase pulse du-

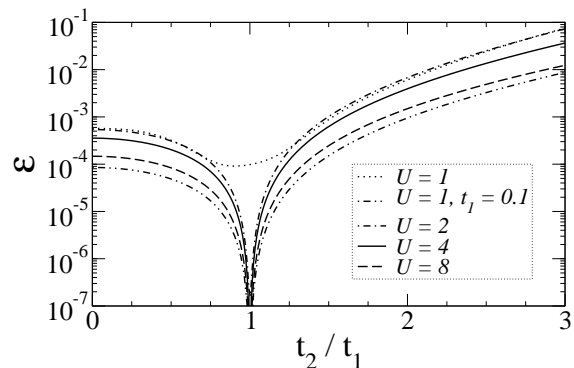


FIG. 3: Full swap error as a function of detuning in the coupling constant t_2 . The parameters used in the pulse width optimization are the same as in Fig. 2. Results for different charging energies are shown.

ration. This is clear in the case of $U = 1$ (see Fig. 2): Even moderate couplings, $t_{1,2} = 0.2$, lead to larger errors, which can then be suppressed by decreasing $t_{1,2}$ by a factor of two; however, that causes a fourfold increase in pulse width which may be problematic in terms of decoherence.

The dependence of errors on fluctuations in the coupling amplitude t_2 is shown in Fig. 3. Again, the pulse duration used is the optimal value obtained when $t_2 = t_1 = 0.2$. As expected, the error grows as t_2 increases. Errors related to large values of t_2 can also be minimized by increasing the switching time, but the same issues raised above appear.

Figure 4 presents the error for two situations involving pulses with duration of about $T/2$, corresponding to the square-root-of-swap operation. The cases shown are: (i) one, and (ii) two consecutive square-root-of-swap pulses. For comparison, the curve corresponding to a full swap pulse is also shown. The error for the square-root-of-swap operation is given by Eq. (6) with $|f\rangle$ replaced by

$$|f'\rangle = \frac{1-i}{2} |S_1\rangle + \frac{1+i}{2} |T_1\rangle. \quad (10)$$

One can observe from Fig. 4 that error rates are nearly the same after a full swap operation and after two consecutive square root of swap operations. This insensitivity of the error to the pulse duration led us to concentrate our effort on the full swap operations.

In order to establish an upper bound for QD tuning accuracy, we have performed simulations where both Δ and t_2 were allowed to vary. The spacing between the levels in QD B was taken from a Gaussian distribution centered at $\bar{\Delta} = 1$, with standard deviation σ_{Δ} ($\epsilon_{N_B}^B = 0$ was kept fixed). For the coupling amplitude, we generated Gaussian distributed level widths $\Gamma_2 = 2\pi t_2^2/\bar{\Delta}$, with average $\bar{\Gamma}_2 = 2\pi t_1^2/\bar{\Delta}$ and standard deviation σ_{Γ_2} . The pulses had their widths optimized for the typical case where $\Delta = \bar{\Delta} = 1$, $U = 4$, $t_{1,2} = 0.2$, and $\tau = 6$. For fixed values of $\bar{\Delta}$, σ_{Δ} , $\bar{\Gamma}_2$, and σ_{Γ_2} , we generated 10,000 realizations of Δ and Γ_2 and each time calculated the error after the application of the full swap pulse. In Fig. 5 we

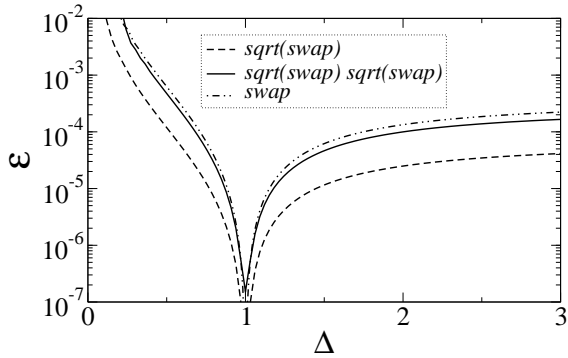


FIG. 4: Comparison of error resulting from a full swap operation and two consecutive square root of swap operations. The error is plotted as a function of upper level detuning in quantum dot B . The pulse width is optimized for $\Delta = 1$, $t_{1,2} = 0.2$, $U = 4$, and $\tau = 6$. The error for a single square-root-of-swap operation is also shown.

show how the probability of having an error larger than the 10^{-4} threshold depends on the energy level accuracy, σ_{Δ} . Two cases are considered, namely, plain and limited control of the inter-dot coupling constant ($\sigma_{\Gamma_2} = 0$ and $0.1\bar{\Gamma}_2$, respectively). The data indicates that frequent, non-correctable errors will happen if an accuracy in Δ of better than 10 percent is not achieved.

B. Relevance for Real Quantum Dots

To make a quantitative estimate of the impact of these results, let us consider the double QD setup of Jeong and coworkers.²⁵ In their device, each QD holds about 40 electrons and has a lithographic diameter of 180 nm (we estimate the effective diameter to be around 120 nm, based on the device electron density). The charging energy and mean level spacing of each QD are approximately 1.8 meV and 0.4 meV, respectively (thus $U/\bar{\Delta} \approx 4.5$). If we allow for a maximal inter-dot coupling of $t_{1,2} \approx 0.2\bar{\Delta}$ (which yields a level broadening of about $0.25\bar{\Delta}$), we find minimal full swap pulse widths of about 100 ps. These values match those used in Fig. 5. For this case, switching times of 10 ps would be long enough to operate in the adiabatic regime and also provide an efficient and well-defined pulse shape. Thus, the combined times should allow for 8-10 consecutive full swap gates before running into dephasing effects related to orbital degrees of freedom.²⁶ While these numbers are yet too small for large-scale quantum computation, they could be sufficient for the demonstration of QD spin qubits. Based on Fig. 5, we find that accuracies in Γ_2 of about 10% would make operations only limited by dephasing, and not by fluctuation-induced errors. However, as shown in the inset, even for small QDs (typically having small $U/\bar{\Delta}$ ratios), the occurrence of large errors is quite frequent when level detuning is large.

An important issue for multi-electron QDs is their strong mesoscopic, sample-to-sample fluctuations in en-

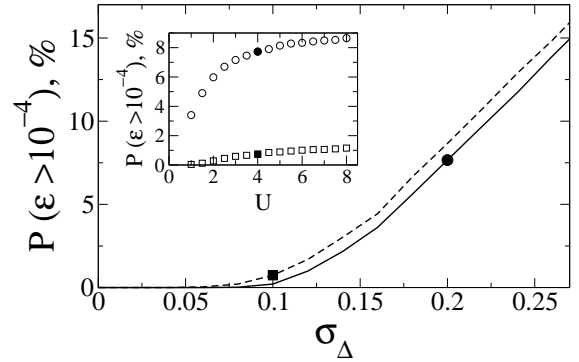


FIG. 5: Probability of having excessively large full swap errors (percentage) as a function of level spacing detuning. The solid (dashed) line corresponds to $\sigma_{\Gamma_2}/\bar{\Gamma}_2 = 0$ (0.1) at $U = 4$ and $t_1 = 0.2$. The inset shows how the probability varies for a fixed width pulse ($T \approx 90$), but different charging energies U , when there is a large level-position detuning: $\sigma_{\Delta} = 0.2$, $\sigma_{\Gamma_2} = 0$ (circles) and moderate level-position and coupling detunings: $\sigma_{\Delta} = 0.1$, $\sigma_{\Gamma_2}/\bar{\Gamma}_2 = 0.1$ (squares).

ergy level position and wave-function amplitudes. Our results so far indicate how big an effect a given change in energy or wave-function will produce; now we go further and discuss how mesoscopic fluctuations more generally affect a collection of qubits.

In experiments, several electrodes are placed around the QD surroundings and their voltages are used to adjust the lateral confining potential, the inter-dot coupling, and the coupling between QDs and leads. These voltages are external parameters that can be used to mitigate the effects of mesoscopic fluctuations by tuning energy levels and wave-functions to desired values. Having that in mind, our results indicate two different scenarios for QD qubit implementations.

First, if one is willing to characterize each QD pair separately and have them operate one by one, mesoscopic fluctuations will be irrelevant. It will be possible, with a single parameter per QD, say, to isolate and align energy levels reasonably well. Errors can be further minimized by decreasing the inter-dot coupling (thus increasing T). But since QDs are not microscopically identical, each pair of QDs will require a different pulse shape and duration. Multi-electron QDs are tunable enough, easy to couple, and much easier to fabricate than one-electron dots; therefore, multi-electron QDs are most appropriate for this case.

Second, if the goal is to achieve genuine scalability, one has to operate qubits in a similar and uniform way, utilizing a single pulse source. In this case, T and τ should be the same for all QD pairs. Based on our results above, one should strive to maximally separate the top most occupied state from all other states, occupied or empty, so as to reduce the possibility of leakage during operations with a fixed duration. At the same time, it is important to reduce inter-pair cross-talk induced by capacitive coupling between electrodes, as well as all inter-dot couplings except between the top most states of each QD.

One should bear in mind that not all electrodes act independently – in most cases a search in a multidimensional parameter space has to be carried out. Thus, four tuning parameters per QD may be necessary to achieve the following goals: (i) find isolated, single-occupied energy level (two parameters); (ii) align this level with the corresponding level in an adjacent QD (one parameter); (iii) control the inter-dot coupling (one parameter). For parameters involved in (i) and (ii), an accuracy of a few percent will likely be required. Finally, control over the inter-dot coupling parameter, (iii), must allow for the application of smooth pulse shapes in the picosecond range. Our simulations also show that the pulse width must be controlled within at least 0.5% accuracy. Although these requirements seem quite stringent, recent experiments indicate that they could be met.²⁷

V. CONCLUSIONS

In summary, our analysis indicate that mid-size QDs, with ten to a few tens of electrons, while not allowing

for extremely fast gates, are still good candidates for spin-qubits. They offer the advantage of being simpler to fabricate and manipulate, but at the same time require accurate, simultaneous control of several parameters. Errors related to detuning and sample-to-sample fluctuations can be large, but can be kept a secondary concern with respect to dephasing effects provided that a sufficient number of independent electrodes or tuning parameters exists.

Acknowledgments

We thank D. P. DiVincenzo, C. M. Marcus, and G. Usaj for useful discussions. This work was supported in part by the National Security Agency and the Advanced Research and Development Activity under ARO contract DAAD19-02-1-0079. Partial support in Brazil was provided by Instituto do Milênio de Nanociência, CNPq, FAPERJ, and PRONEX.

-
- ¹ P. W. Shor, in *Proceedings of the 35th Annual Symposium on Foundations of Computer Science* (IEEE Computer Society Press, Los Alamitos, CA, 1994), p. 124.
- ² L. K. Grover, in *Proceedings of the 28th Annual ACM Symposium on Theory of Computing* (Association for Computing Machinery Press, New York, 1996), p. 212.
- ³ D. Loss and D. P. DiVincenzo, *Phys. Rev. A* **57**, 120 (1998).
- ⁴ A. Barenco, C. H. Bennett, R. Cleve, D. P. DiVincenzo, N. Margolus, P. Shor, T. Sleator, J. A. Smolin, and H. Weinfurter, *Phys. Rev. A* **52**, 3457 (1995).
- ⁵ D. P. DiVincenzo, G. Burkard, D. Loss, and E. V. Sukhorukov, in *Quantum Mesoscopic Phenomena and Mesoscopic Devices in Microelectronics*, edited by I. O. Kulik and R. Ellialtioglu (Kluwer, 2000).
- ⁶ D. P. DiVincenzo, *Phys. Rev. A* **51**, 1015 (1995).
- ⁷ D. P. DiVincenzo, D. Bacon, J. Kempe, G. Burkard, and K. B. Whaley, *Nature* **408**, 339 (2000).
- ⁸ C. M. Marcus (private communication).
- ⁹ X. Hu and S. Das Sarma, *Phys. Rev. A*, **64**, 042312 (2001).
- ¹⁰ G. Burkard, D. Loss, and D. P. DiVincenzo, *Phys. Rev. B* **59**, 2070 (1999).
- ¹¹ X. Hu and S. Das Sarma, *Phys. Rev. A* **61**, 062301 (2000); *ibid.* **66**, 012312 (2002).
- ¹² X. Hu, R. de Sousa, and S. Das Sarma, *Phys. Rev. Lett.* **86**, 918 (2001).
- ¹³ J. Schliemann, D. Loss, and A. H. MacDonald, *Phys. Rev. B* **63**, 085311 (2001).
- ¹⁴ T. Brandes and T. Vorrath, *Phys. Rev. B* **66**, 075341 (2002).
- ¹⁵ L. P. Kouwenhoven, C. M. Marcus, P. L. McEuen, S. Tarucha, R. M. Westervelt, and N. S. Wingreen, in *Mesoscopic Electron Transport*, edited by L. L. Sohn, L. P. Kouwenhoven, and G. Schön (Kluwer, Dordrecht, 1997).
- ¹⁶ I. L. Aleiner, P. W. Brouwer, and L. I. Glazman, *Phys. Rep.* **358**, 309 (2002).
- ¹⁷ D. Ullmo and H. U. Baranger, *Phys. Rev. B*, **64**, 245324 (2001).
- ¹⁸ G. Usaj and H. U. Baranger, *Phys. Rev. B*, **64**, 201319(R) (2001); *ibid.* **66**, 155333 (2002); *ibid.* **67**, 121308(R) (2003).
- ¹⁹ D. Ullmo, T. Nagano, S. Tomsovic, and H. U. Baranger *Phys. Rev. B* **63**, 125339 (2001).
- ²⁰ L. P. Kouwenhoven, D. G. Austing, and S. Tarucha, *Rep. Prog. Phys.* **64**, 701 (2001).
- ²¹ Though we assume time-reversal symmetry (real t_1 and t_2), we have checked that its violation does not modify our results.
- ²² While such states can lead to the full spin swap (with probability equal to 1/2), they will induce severe detuning errors in subsequent operations.
- ²³ A. Steane, *Rep. Prog. Phys.* **61**, 117 (1998).
- ²⁴ See, *e.g.*, W. H. Press, B. P. Flannery, S. A. Teukolsky, and W. T. Vetterling, *Numerical Recipes in Fortran* (Cambridge University Press, 2nd edition, 1992).
- ²⁵ H. Jeong, A. M. Chang, and M. R. Melloch, *Science* **293**, 2221 (2001).
- ²⁶ T. Hayashi, T. Fujisawa, H. D. Cheong, Y. H. Jeong, and Y. Hirayama, *Phys. Rev. Lett.* **91**, 226804 (2003).
- ²⁷ J. C. Chen, A. M. Chang, and M. R. Melloch, preprint (cond-mat/0305289).